AGU PUBLICATIONS

JGR

Journal of Geophysical Research: Atmospheres

RESEARCH ARTICLE
10.1002/2014JD022463

Key Points:
- A bipolar flash containing one positive and five negative strokes is presented
- The downward positive leader preceding the first stroke propagates quiet fast
- Detailed optical progression characteristics of leader-return stroke are given

Correspondence to:
W. Lu,
wtlu@cams.cma.gov.cn

Citation:
Chen, L., W. Lu, Y. Zhang, and D. Wang (2015), Optical progression characteristics of an interesting natural downward bipolar lightning flash, *J. Geophys. Res. Atmos.*, *120*, 708–715, doi:10.1002/2014JD022463.

Received 20 AUG 2014
Accepted 24 DEC 2014
Accepted article online 6 JAN 2015
Published online 31 JAN 2015

Optical progression characteristics of an interesting natural downward bipolar lightning flash

Luwen Chen[1,2,3,4], Weitao Lu[1,2,3], Yijun Zhang[1,2,3], and Daohong Wang[5]

[1]State Key Laboratory of Severe Weather, Chinese Academy of Meteorological Sciences, Beijing, China, [2]Collaborative Innovation Center on Forecast and Evaluation of Meteorological Disasters, Nanjing University of Information Science and Technology, Nanjing, China, [3]Laboratory of Lightning Physics and Protection Engineering, Chinese Academy of Meteorological Science, Beijing, China, [4]Lightning Protection Center of Guangdong Province, Guangzhou, China, [5]Department of Electrical and Electronic Engineering, Gifu University, Gifu, Japan

Abstract Using high-speed cameras, Lightning Attachment Process Observation Systems, and fast and slow electrical antennas, we documented a downward bipolar lightning flash that contained one first positive stroke with a peak current of 142 kA and five subsequent negative strokes hitting on a 90 m tall structure on 29 July 2010 in Guangzhou City, China. All the six strokes propagated along the same viewed channel established by the first positive return stroke. The leader which preceded the positive return stroke propagated downward without any branches at a two-dimensional (2-D) speed of 2.5×10^6 m/s. An upward connecting leader with a length of about 80 m was observed in response to the downward positive leader. The 10–90% risetimes of the return strokes' optical pulses ranged from 2.2 μs to 3.2 μs, while the widths from the 10% wavefront to the 50% wave tail ranged from 56.5 μs to 83.1 μs, and the half peak widths ranged from 53.4 μs to 81.6 μs. All the return strokes exhibited similar speeds, ranging from 1.0×10^8 m/s to 1.3×10^8 m/s. Each of the return strokes was followed by a continuing current stage (CC). The first positive stroke CC lasted more than 150 ms, much larger than all the subsequent negative stroke CC, ranging from 13 ms to 70 ms.

1. Introduction

Bipolar lightning, in which both positive and negative charges are transferred to the ground in a single lightning flash, has been reported by many authors. *Hagenguth and Anderson* [1952] found that bipolar lightning flashes account for approximately 14% of the total lightning flashes striking the Empire State Building. *Berger* [1978] reported that 6% of lightning flashes observed at Mount San Salvatore are bipolar. *Jerauld et al.* [2004] presented current, luminosity, and electric and magnetic field measurements for a triggered lightning flash containing both negative and positive strokes. Based on a review of the literature, *Rakov* [2005] deduced that bipolar flashes constitute 6–14% of summer lightning in Europe and the United States and 3–33% of winter lightning in Japan when tall objects are involved.

Based on the characteristics of the current polarity reversal, *Rakov* [2003] divided bipolar lightning flashes into three categories: Type 1 bipolar flashes are characterized by a current and charge polarity reversal during the initial stage of a natural upward or rocket-triggered lightning discharge, Type 2 bipolar flashes involve a polarity change in current and charge between the initial stage of a natural upward or rocket-triggered lightning discharge and the return strokes following the initial stage, and Type 3 bipolar flashes are associated with a polarity reversal between subsequent return strokes. *Jerauld et al.* [2009] divided the Type 3 bipolar flashes into two subcategories, with Type 3a events being natural upward or rocket-triggered lightning discharges and Type 3b events being natural downward cloud-to-ground flashes.

Most reported bipolar flashes correspond to Types 1, 2, and 3a, while Type 3b events are relatively rare. *Jerauld et al.* [2009] presented electrical, magnetic, and video records of a natural downward cloud-to-ground lightning flash containing two positive strokes followed by four negative strokes. *Fleenor et al.* [2009] reported four bipolar flashes captured on video and corresponding National Lightning Detection Network records. *Saba et al.* [2012] presented observations of two single-channel bipolar cloud-to-ground flashes. Recently, *Saraiva et al.* [2014] presented high-speed video and electromagnetic analysis of two natural bipolar cloud-to-ground lightning flashes. In this paper, simultaneous records obtained from two high-speed cameras, two Lightning Attachment Process Observation Systems (LAPOSs), and flat-plate electrical antennas for a single natural downward bipolar flash observed in 2010 will be presented and analyzed.

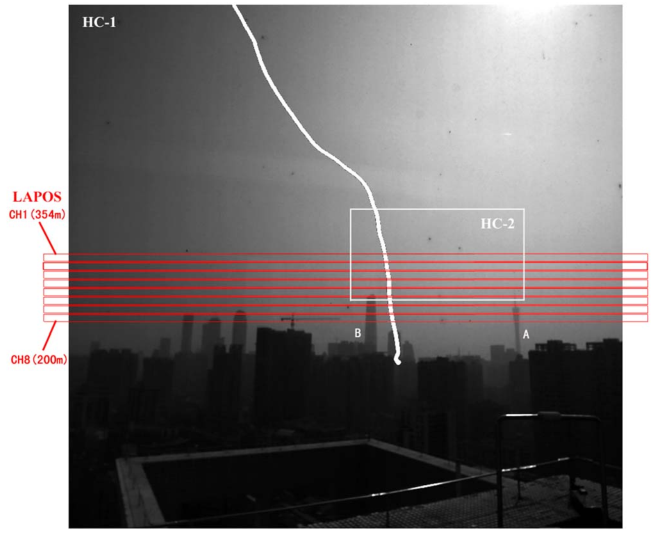

Figure 1. Composed image of the lightning channel of F1010 and the field of view of the HC-1. The symbols "A" and "B" indicate the top two tallest structures in the field of view, the eight (CH1-CH8) strips indicate the field of view of the LAPOSs, and the white rectangle indicates the field of view of the HC-2.

2. Experiment and Equipment

A field experiment focusing on lightning flashes striking tall structures has been ongoing since 2009 in Guangzhou, Guangdong Province, China [e.g., *Lu et al.*, 2012, 2013]. The observation site is located on a structure with a height of approximately 100 m at the Guangdong Meteorological Bureau. Several instruments were used to simultaneously measure the acoustic, optical, electric, and magnetic field signals produced by lightning discharges. A microphone array consisting of four microphones was used to record the acoustic signals of nearby lightning. For the case presented in this paper, two Photron Fastcam SA5 high-speed cameras were used to capture the images of the lightning flashes. One high-speed camera, HC-1, equipped with a color sensor and a 14 mm lens, was set at a sampling rate of 10,000 frames per second (fps), a resolution of 896 × 848 pixels, a recording duration of 0.8 s, and a 10% pretrigger time. Another high-speed camera, HC-2, equipped with a monochrome sensor and a 20 mm lens, was set at a sampling rate of 50,000 fps, a resolution of 512 × 272 pixels, a recording duration of 0.5 s, and a 2% pretrigger time. Two Lightning Attachment Process Observation Systems (LAPOSs), each consisting of a 16 mm lens, a camera body, an optical fiber array, eight photodiodes, and eight amplifiers [*Wang et al.*, 2011], were installed to observe optical signals of the attachment process within the field of view. One LAPOS, LAPOS1, with higher sensitivity is suitable for detecting the luminosity variations produced by the lightning leader, while the other LAPOS, LAPOS2, with lower sensitivity is suitable for monitoring the luminosity variations induced by the lightning return strokes. Each LAPOS has a horizontal view angle of about 127° and a vertical view angle of about 1°. Figure 1 shows the composed image of the lightning channel of F1010 and the field of view of the LAPOSs, the HC-1, and the HC-2. The vertical center of the field of view of the LAPOSs was aimed at the top of structure A, and the horizontal view range was adjusted to cover both structures A and B. A flat-plate fast antenna and a flat-plate slow antenna, with time constants of 1 ms and 6 s, respectively, were used to obtain the electric field change produced by the lightning discharge. The signals from the LAPOSs, the fast antenna, and the slow antenna were recorded by two YOKOGAWA DL750 digital oscilloscopes with a sampling rate of 10 MHz. One channel of LAPOS2 was used as a trigger source for all of the instruments. For each triggering event, the GPS time of the triggering signal, with an accuracy of 30 ns, was provided by a high-precision GPS timing system. The peak current values of the return lightning strokes were obtained from records of the Guangdong Power Grid Lightning Location System. According to the performance evaluation for the Guangdong Power Grid Lightning Location System based on observations of artificially triggered lightning and natural lightning flashes [*Chen et al.*, 2012], the arithmetic mean value of flash detection efficiency, stroke detection efficiency, location error, and absolute percentage errors of peak current estimation are about 94%, 60%, 710 m, and 16.3%, respectively.

3. Data and Analysis

3.1. Overview

The natural downward bipolar flash studied in this paper occurred at 09:54:14 UTC, 29 July 2010. This flash, numbered F1010 in our tall-object lightning data set, began with a positive stroke followed by five subsequent negative strokes. This event is the only bipolar lightning flash that has been recorded from 2009 to the present. Figure 2 shows the simultaneous records obtained by the slow antenna and fast antenna. The duration of F1010 was approximately 864 ms, and the interstroke intervals were 278 ms, 76 ms, 111 ms, 78 ms, and 149 ms, respectively. The records of HC-1 indicate that the first and subsequent strokes hit the top of a structure with a

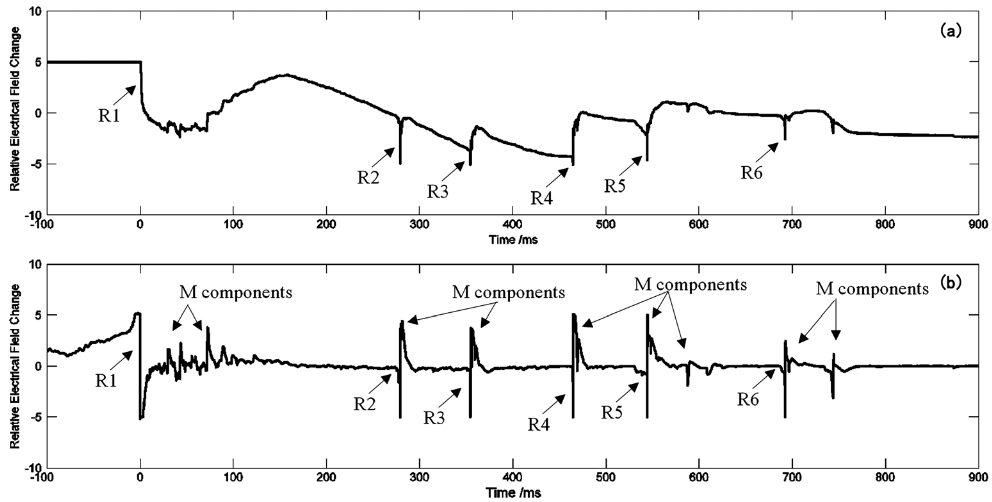

Figure 2. Simultaneous records of (a) the slow antenna and (b) the fast antenna. Time 0 is set at the occurrence of the first return stroke.

height of approximately 90 m located approximately 1200 m from the observation site (see Figure 1), following the same channel to ground established by the first return stroke. Five return strokes (R1, R2, R3, R4, and R5) with peak current values of 142.0, −24.5, −22.9, −32.0, and −30.6 kA, respectively, were recorded by the Guangdong Power Grid Lightning Location System, while the sixth return stroke, with a relatively weak amplitude, was missed.

3.2. Characteristics of the First Positive Leader-Return Stroke Process

Figure 2a shows that the slow electrical antenna record was positively saturated during the 100 ms before the first positive return stroke. The waveform of the fast electrical antenna record (Figure 2b) exhibited a positive variation after approximately −79 ms, followed by a monotonically increasing trend produced by the descending positive leader beginning at approximately −14 ms; the record became saturated at −5.2 ms. It can be determined from the results described above that there exist significant intracloud discharge activities preceding the first positive return stroke of F1010, which is similar to the situation indicated by *Rust et al.* [1981] and *Fuquay* [1982] in their observations of positive return strokes.

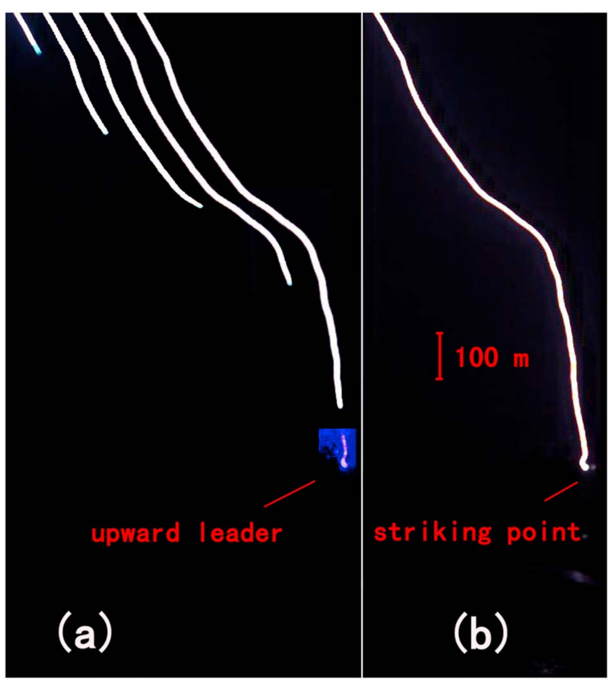

Figure 3. Images of downward positive leader and upward negative leader captured by HC-1: (a) for the five images before the R1 and (b) for the one image of the lightning channel after the R1. The brightness and contrast of the upward negative leader are enhanced for a better view.

Figure 3 shows the last five images of downward positive leader captured by HC-1, with a two-dimensional (2-D) resolution of approximately 1.7 m per pixel for the lightning channel of F1010. The image of the downward positive leader was first captured at approximately −0.5 ms by HC-1, when the distance from the

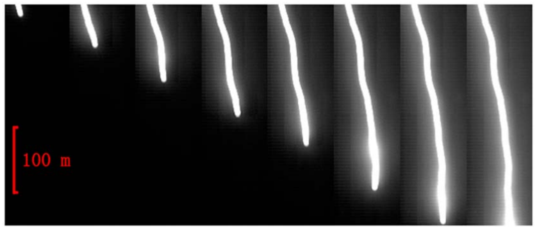

Figure 4. Eight images of downward positive leader before the R1 captured by HC-2.

leader tip to the strike point was estimated to be approximately 1074 m. From Figure 3, it can be found that in the 2-D image, the positive leader propagated in a downward slanted direction from −0.5 ms to −0.3 ms and then turned to an almost vertical downward direction at approximately −0.2 ms; at that time, the distance between the tip of the positive leader and the strike point was approximately 600 m. Unlike most natural downward negative stepped leaders, the first positive leader of F1010 did not exhibit any branches within the field of view of HC-1. Four partial 2-D propagation speeds with a range from 2.1×10^6 m/s to 3.0×10^6 m/s and an arithmetic mean of 2.5×10^6 m/s were deduced from Figure 3a. In the fifth image of Figure 3a, an upward negative connecting leader initiated from the top of the structure struck by F1010 can be seen just before R1, for which the 2-D length was approximately 80 m and the 2-D distance between the tips of the downward leader and the upward connecting leader was approximately 79 m. Thus, it could be deduced that the 2-D propagation speeds of the upward negative connecting leader were smaller than 8.0×10^5 m/s before R1.

Figure 4 shows eight images of downward positive leader before the R1 captured by HC-2, with a 2-D resolution of approximately 1.2 m per pixel for the lightning channel of F1010. The field of view of HC-2 was relatively small, in which the distance from the tip of the downward leader to the strike point was estimated to be within the range of 218 m to 542 m. Six partial 2-D propagation speeds with a range of 2.4×10^6 m/s to 3.4×10^6 m/s and an arithmetic mean of 2.7×10^6 m/s were deduced from Figure 4. It can be determined from Figure 4 that the brightest section of the downward positive leader occurred at a distance on the order of tens of meters from the tip of the leader.

Figure 5 presents the records of LAPOS1 and LAPOS2 for the first leader-return stroke process. Note that the CH3 and CH6 waveforms of both LAPOSs were not recorded due to the limitation of channel numbers of DL750. The vertical one-dimensional (1-D) spatial resolution of the LAPOS records for the trajectory of F1010 is estimated to be approximately 22 m per channel. It can also be deduced that the trajectory of F1010 is approximately vertical in the field of view of both LAPOSs. As shown in Figure 5a, a luminosity pulse produced by the downward leader first occurred at approximately −108 μs in the Ch1 waveform and then propagated sequentially according to the channel numbers. Pulses appeared in the waveform records from −70 μs to −10 μs, with a fluctuation period ranging between 10 and 16 μs, indicating that the positive leader is a stepped one, like that reported by *Wang and Takagi* [2011]. The average 1-D propagation speed of the downward positive leader of F1010 was estimated to be approximately 2.4×10^6 m/s according to the records of LAPOS1, which is very similar to that derived from the records of HC-1 and HC-2. It can be seen that the record of LAPOS1 was saturated when the first stroke occurred due to the limitation of the dynamic range.

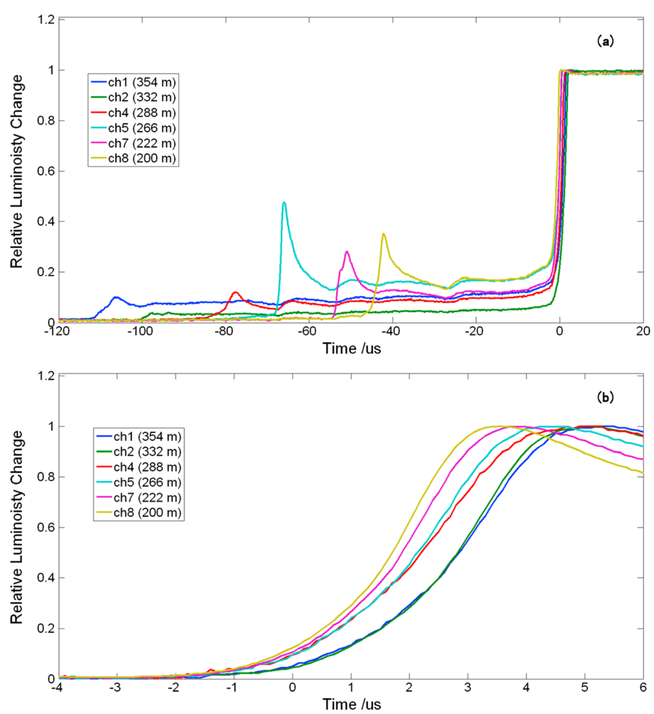

Figure 5. Records obtained from (a) LAPOS1 and (b) LAPOS2 for the first leader-return stroke process of F1010. Time 0 is set at the occurrence of the first return stroke.

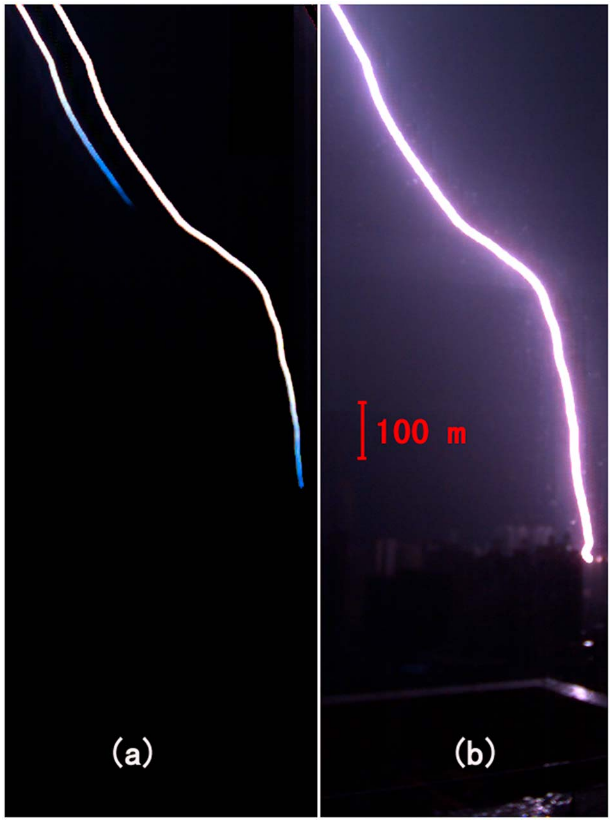

Figure 6. Images of downward negative leader captured by HC-1: (a) for the two images before the R2 and (b) for the one image of the lightning channel after the R2.

Saba et al. [2008] reported that the partial 2-D propagation speeds of positive leaders range from 2.3×10^4 m/s to 1.3×10^6 m/s, with a mean value of 2.5×10^5 m/s, based on 39 samples observed by high-speed cameras. *Berger and Vogelsanger* [1966] reported that the partial 2-D propagation speeds of positive leaders can be as high as 2.4×10^6 m/s. Compared with the above results, the maximum value of the 2-D propagation speed of the positive leader of F1010 was in the upper end of the positive leader speeds reported in the literatures.

The 10–90% risetime of the optical pulses produced by R1 in Figure 5b is estimated to be approximately 3.2 μs, while the width from the 10% wavefront to the 50% wave tail and the half peak width are approximately 56.1 μs and 53.4 μs, respectively. From the time difference of the light signals in Figure 5b, we estimated that the upward propagation speed of R1 was approximately 1.0×10^8 m/s.

Following R1, a continuing current lasting more than 150 ms was identified by visual inspection based on the records of HC-1. Several weak luminosity pulses coinciding with the pulses indicated by the fast antenna waveform were also found superimposed on the continuing currents, which are believed to be produced by the *M*-component processes. Continuing currents with a duration of 90 ms and 71 ms following the first positive stroke were also found in the two bipolar cloud-to-ground flashes reported by *Saba et al.* [2012], while *Jerauld et al.* [2009] found that the continuing current following the second positive stroke has a duration of at least 400 ms. The observations mentioned above were consistent with the point that positive lightning strokes tend to be followed by continuing currents that typically last for tens to hundreds of milliseconds.

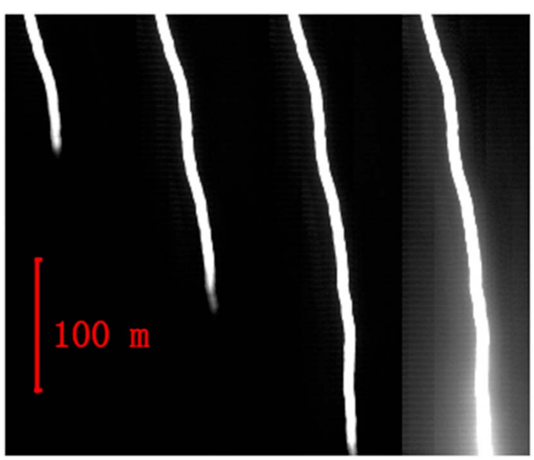

Figure 7. Four images of the subsequent downward negative leader before the R2 captured by HC-2.

3.3. Characteristics of the Subsequent Negative Leader-Return Stroke Process

Figure 6 shows two images of the subsequent downward negative leader before R2 captured by HC-1, while Figure 7 shows four images of the subsequent downward negative leader before the R2 captured by HC-2. From Figure 6, one partial 2-D propagation speed with the value of 6.6×10^6 m/s can be estimated for the subsequent downward negative leader before R2, which is very close to the value of 6.5×10^6 m/s derived from the records of HC-2.

Figure 8 presents the records of LAPOS1 and LAPOS2 for the subsequent leader-return stroke process of R2. In Figure 8a, the luminosity pulses produced by the subsequent downward negative

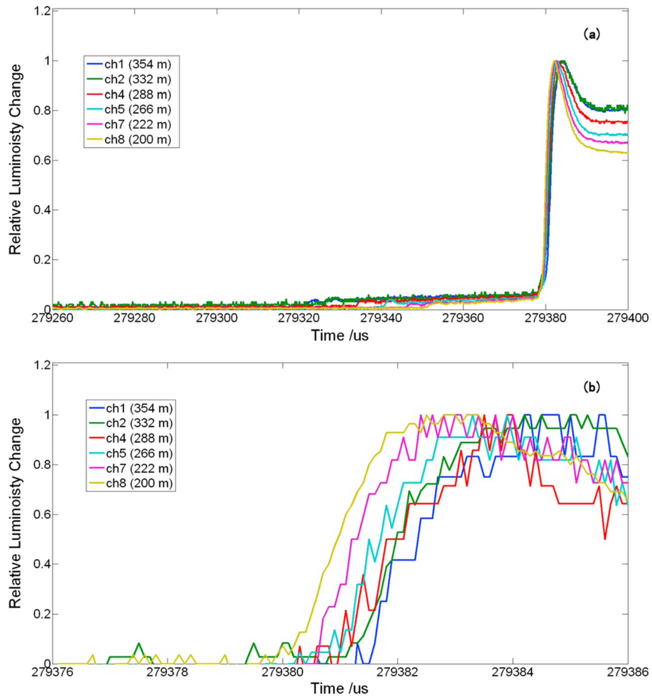

Figure 8. Records obtained from (a) LAPOS1 and (b) LAPOS2 for the subsequent leader-return stroke process of F1010. Time 0 is set at the occurrence of the first return stroke.

leader were much weaker than those produced by the positive leader, as indicated in Figure 5a. This situation makes it difficult to estimate the 1-D propagation speed of the subsequent downward negative leader of F1010 based on the records of LAPOSs. However, an apparent upward propagation optical phenomenon produced by the R2 return stroke process can be distinguished in Figure 8b, and the 1-D speed of the return stroke can be estimated to be about 1.3×10^8 m/s. In addition, the 10–90% risetime of the optical pulses induced by R2 is estimated to be approximately 2.3 μs, while the width from the 10% wavefront to the 50% wave tail and the half peak width are approximately 70.5 μs and 69.0 μs, respectively. Similarly, we have performed relevant measurements for R3, R4, R5, and R6, and all the results are summarized in Table 1.

Note that only the records of HC-2 were used to estimate the 2-D propagation speeds of the downward leaders before R3 and R4 because no 2-D partial speeds could be discriminated from the records of HC-1. The processes of R5 and R6 were missed by HC-2 due to limitations on the recording duration. The HC-1 records show that the tip of the negative downward leader was outside the field of view of HC-1 at 0.1 ms before R5; thus, it can be inferred that the 2-D propagation speed of the downward leader before R5 is greater than 12.4×10^6 m/s. It seems that the 2-D speeds of the downward leaders prior to each subsequent return stroke were characterized by a successive rising trend from R2 to R5 and then dropped significantly for R6.

The records of HC-1 or HC-2 also showed that the subsequent downward negative leaders exhibited a weaker luminosity compared to the first positive downward leader, which may explain the difficulty encountered in discriminating the 1-D propagation speeds of those negative leaders via the LAPOS records.

The 1-D speeds of the negative subsequent return strokes were found to be within the range of 1.2×10^8 m/s to 1.3×10^8 m/s according to the records of LAPOS1 and LAPOS2, which is slightly greater than that of R1. The 10–90% risetimes of the optical pulses induced by the negative subsequent return strokes were found to be within a range of 2.2 μs to 2.6 μs. The widths from the 10% wavefront to the 50% wave tail were found to

Table 1. Summary of Parameters for the First Positive and the Five Subsequent Negative Leader-Return Stroke Processes of F1010

		Return Stroke				
Return Stroke Number	2-D Speed of the Downward Leader Prior to the Return Stroke ($\times 10^6$ m/s)	1-D Speed ($\times 10^8$ m/s)	10–90% Risetime of the Optical Pulse (μs)	Width From the 10% Wavefront to the 50% Wave Tail of the Optical Pulse (μs)	Width From the 50% Wavefront to the 50% Wave Tail of the Optical Pulse (μs)	Lightning Location System Reported Peak Current (kA)
R1	2.5	1.0	3.2	56.1	53.4	142.0
R2	6.5	1.3	2.3	70.5	69.0	−24.5
R3	9.2	1.3	2.2	71.3	69.9	−22.9
R4	10.7	1.3	2.5	83.1	81.6	−32.0
R5	>12.4	1.3	2.6	73.7	72.3	−30.6
R6	4.0	1.2	2.6	65.5	64.3	-

range from 65.5 μs to 83.1 μs, and the half peak widths range from 64.3 μs to 81.6 μs. The results show that the 10–90% risetimes of the subsequent return strokes are all shorter than that of R1, while the widths from the 10% wavefront to the 50% wave tail and the half peak widths are greater.

Continuing currents were observed following each negative subsequent return stroke, with durations ranging from 13 to 70 ms based on a visual inspection of the HC-1 records, which is significantly shorter than that following R1. It is worth noting that two to four *M* components were found superimposed on the continuing currents following each subsequent return stroke, with a more intense luminosity pulse than observed for the continuing currents following R1. Additionally, a pulse at approximately 745 ms was observed with a much lower rising time in comparison to the typical negative return stroke process observed for an increasing waveform, which may have been produced by processes similar to an *M* component.

4. Summary

In this paper, we reported a downward bipolar lightning flash that contained one first positive stroke with a peak current of 142 kA and five subsequent negative strokes hitting on a 90 m tall structure on 29 July 2010 in Guangzhou City, China. The results can be summarized in the following:

1. The downward positive leader prior to the first return stroke exhibited a 2-D propagation speed of 2.5×10^6 m/s. Fluctuations were observed in the 2-D partial propagation speeds as well as the leader channel luminosity of the positive leader prior to the first return stroke as the leader approached the ground. Apparently, the positive leader is a stepped one. An upward connecting leader with a length of about 80 m was observed in response to the downward positive leader.
2. The speeds of all the return strokes were similar, ranging from 1.0×10^8 m/s to 1.3×10^8 m/s. The 10–90% risetimes of the return strokes' optical pulses ranged from 2.2 μs to 3.2 μs, while the widths from the 10% wavefront to the 50% wave tail ranged from 56.5 μs to 83.1 μs, and the half peak widths ranged from 53.4 μs to 81.6 μs.
3. The duration of the continuing current following the first return stroke (greater than 150 ms) was much longer than those following the subsequent return strokes (13–70 ms). Several *M* components were found superimposed on the continuing currents following both the first positive return strokes and the subsequent negative return strokes.

Similar to the six single-channel bipolar cloud-to-ground flashes reported in the literatures [*Jerauld et al.*, 2009; *Fleenor et al.*, 2009; *Saba et al.*, 2012; *Saraiva et al.*, 2014], F1010 had the first stroke of positive polarity. *Saba et al.* [2012] conjectured that the preceding positive stroke channel may give rise to recoil leaders and forming subsequent negative strokes. Recently, *Saraiva et al.* [2014] presented the first optical evidence that both single- and multiple-channel bipolar flashes occur as a consequence of recoil leader activity in the branches of the initial positive return stroke. That is why no single-channel bipolar cloud-to-ground flashes have a first stroke of negative polarity. The observation of the case presented in this paper is consistent with the theory.

Acknowledgments
This work was supported in part by the National Natural Science Foundation of China (grant 41475003), the National Key Basic Research Program of China (grant 2014CB441405), and the Basic Research Fund of Chinese Academy of Meteorological Sciences (grants 2014R015 and 2013Z006). The simultaneous optical and electrical observation data for the lightning flash analyzed in this paper can be obtained upon request from Weitao Lu (wtlu@cams.cma.gov.cn).

References

Berger, K. (1978), Blitzstrom-Parameter von Aufwärtsblitzen, *Bull. Schweiz. Elektrotech. Ver.*, *69*, 353–360.

Berger, K., and E. Vogelsanger (1966), Photographische Blitzuntersuchungen der Jahre 1955–1965 auf dem Monte San Salvatore, *Bull. Schweiz. Elektrotech. Ver.*, *57*, 599–620.

Chen, L., Y. Zhang, W. Lu, D. Zheng, Y. Zhang, S. Chen, and Z. Huang (2012), Performance evaluation for a lightning location system based on observations of artificially triggered lightning and natural lightning flashes, *J. Atmos. Oceanic Technol.*, *29*, 1835–1844, doi:10.1175/JTECH-D-12-00028.1.

Fleenor, S. A., C. J. Biagi, K. L. Cummins, E. P. Krider, and X. M. Shao (2009), Characteristics of cloud-to-ground lightning in warm-season thunderstorms in the Central Great Plains, *Atmos. Res.*, *91*, 333–352, doi:10.1016/j.atmosres.2008.08.011.

Fuquay, D. M. (1982), Positive cloud-to-ground lightning in summer thunderstorms, *J. Geophys. Res.*, *87*, 7131–7140.

Hagenguth, J. H., and J. G. Anderson (1952), Lightning to the Empire State Building: Part III, *AIEE Trans.*, *71*, 641–*649*.

Jerauld, J., M. A. Rakov, V. A. Uman, K. J. Rambo, and D. M. Jordan (2004), A triggered lightning flash containing both negative and positive strokes, *Geophys. Res. Lett.*, *31*, L08104, doi:10.1029/2004GL019457.

Jerauld, J., M. A. Uman, V. A. Rakov, K. J. Rambo, D. M. Jordan, and G. H. Schnetzer (2009), Measured electric and magnetic fields from an unusual cloud-to-ground lightning flash containing two positive strokes followed by four negative strokes, *J. Geophys. Res.*, *114*, D19115, doi:10.1029/2008JD011660.

Lu, W., L. Chen, Y. Zhang, Y. Ma, Y. Gao, Q. Yin, S. Chen, Z. Huang, and Y. Zhang (2012), Characteristics of unconnected upward leaders initiated from tall structures observed in Guangzhou, *J. Geophys. Res.*, *117*, D19211, doi:10.1029/2012JD018035.

Lu, W., L. Chen, Y. Ma, V. A. Rakov, Y. Gao, Y. Zhang, Q. Yin, and Y. Zhang (2013), Lightning attachment process involving connection of the downward negative leader to the lateral surface of the upward connecting leader, *Geophys. Res. Lett.*, *40*, 5531–5535, doi:10.1002/2013GL058060.

Rakov, V. A. (2003), A review of positive and bipolar lightning discharges, *Bull. Am. Meteorol. Soc.*, 767–775, doi:10.1175/BAMS-84-6-767.
Rakov, V. A. (2005), Lightning flashes transporting both negative and positive charges to ground, in *Recent Progress in Lightning Physics*, edited by C. Pontikis, pp. 9–21, Research Signpost, Kerala, India.
Rust, W. D., D. R. MacGorman, and R. T. Arnold (1981), Positive cloud-to-ground lightning flashes in severe storms, *Geophys. Res. Lett.*, *8*, 791–794.
Saba, M. F., K. L. Cummins, T. A. Warner, E. P. Krider, L. Z. S. Campos, M. G. Ballarotti, O. Pinto Jr., and S. A. Fleenor (2008), Positive leader characteristics from high-speed video observations, *Geophys. Res. Lett.*, *35*, L07802, doi:10.1029/2007GL033000.
Saba, M. F., C. Schumann, T. A. Warner, W. Schulz, and R. E. Orville (2012), Bipolar cloud-to-ground flashes observations, paper presented at 32th International Conference on Lightning Protection, Vienna, Austria.
Saraiva, A. C. V., et al. (2014), High-speed video and electromagnetic analysis of two natural bipolar cloud-to-ground lightning flashes, *J. Geophys. Res. Atmos.*, *119*, 6105–6127, doi:10.1002/2013JD020974.
Wang, D., and N. Takagi (2011), A downward positive leader that radiated optical pulses like a negative stepped leader, *J. Geophys. Res.*, *116*, D10205, doi:10.1029/2010JD015391.
Wang, D., T. Watanabe, and N. Takagi (2011), A high speed optical imaging system for studying lightning attachment process, in Proceedings of the 7th Asia-Pacific International Conference on Lightning, Chengdu, China, pp. 937–940.